

Description of carbon isotopes within relativistic Hartree-Fock-Bogoliubov theory

Xiao Li Lu (卢小丽), Bao Yuan Sun (孙保元), and Wen Hui Long (龙文辉)*

School of Nuclear Science and Technology, Lanzhou University, 730000 Lanzhou, China

(Received 21 October 2012; revised manuscript received 13 February 2013; published 7 March 2013)

Within the relativistic Hartree-Fock-Bogoliubov (RHFB) theory, the structure properties of carbon isotopes are systematically studied. To provide better overall description, the finite-range Gogny force D1S with an adjusted strength factor is adopted as the effective pairing interaction in the particle-particle channel. The self-consistent RHFB calculations with density-dependent meson-nucleon couplings indicate the single-neutron halo structures in both ^{17}C and ^{19}C , whereas the two-neutron halo in ^{22}C is not well supported. It is also found that close to the neutron drip line there exists distinct odd-even staggering on neutron radii, which is tightly related with the blocking effects, and correspondingly the blocking effect plays a significant role in the single-neutron halo formation.

DOI: [10.1103/PhysRevC.87.034311](https://doi.org/10.1103/PhysRevC.87.034311)

PACS number(s): 21.60.Jz, 21.10.Dr, 21.30.Fe, 27.20.+n

I. INTRODUCTION

During past decades, radioactive ion beams (RIBs) have greatly extended our knowledge of nuclear physics, from which the critical data for nuclear physics, astrophysics, and testing the standard model are obtained. With worldwide and rapid development of RIB facilities, investigations of nuclear systems under extreme conditions generate new frontiers in nuclear physics. For example, the exotic nuclei [1–4] have attracted interest due to their unexpected exotic modes. One of the representatives is the nuclear halo structure, characterized by a dilute matter distribution contributed to by several (in general, two) loosely bound valence neutrons (or protons) surrounding a condensed core, which was first found in ^{11}Li [5]. As typical light nuclei, carbon isotopes have been used to probe possible halo structure [6–8], and the recently measured reaction cross section of ^{22}C [9] seems to support a two-neutron halo structure, which has also attracted fairly large interest from the community [10–12].

In fact, the exotic modes found in weakly bound nuclear systems also bring serious challenges to the reliability of nuclear theoretical models. When extended to the limit of stability of isotopes or isotones, the single neutron or proton separation energies become comparable to the pairing gap energy, such that the continuum effects can be easily involved by pairing correlations and play a significant role in determining the structure properties of exotic nuclei [13–15]. In terms of the Bogoliubov quasiparticle, the relativistic Hartree-Bogoliubov (RHB) theory [15–17] has unified the descriptions of relativistic Hartree (RH) mean field and pairing correlations, and consequently the continuum effects are involved automatically. Since the first self-consistent description of nuclear halo structure in ^{11}Li [13], the RHB theory has been successfully applied in predicting the giant halos in Ca [18,19] and Zr [14,19,20] isotopes, as well as the restoration of relativistic symmetry [21] and superheavy magic structures [22].

With the inclusion of Fock terms in the mean field, the relativistic Hartree-Fock-Bogoliubov (RHFB) theory with density-dependent meson-nucleon couplings [23] provides a self-consistent platform for the exploration of exotic nuclei, e.g., predicting the giant halos in cerium isotopes [19]. In addition, the inclusion of Fock terms has brought substantial improvements in the self-consistent description of nuclear shell structures [24] and evolutions [25,26], relativistic symmetry restorations [24,27,28], and low-energy excitation modes [29].

In this work, the structural properties of carbon isotopes, particularly the possible halo structures therein, are studied systematically within the RHFB and RHB theories. The contents are organized as follows. In Sec. II, we introduce the general formalism of the RHFB equations with finite-range (Gogny) pairing force. In Sec. III, the discussions are concentrated on the halo structures and odd-even staggering (OES) on the neutron radii for carbon isotopes. Finally, a brief summary and perspective are given in Sec. IV.

II. THEORETICAL FRAMEWORK AND NUMERICAL DETAILS

In relativistic nuclear models the effective force between the nucleons is mediated by the exchange of mesons and photons. Based on that, the model Lagrangian contains the system degrees of freedom associated with the nucleon ψ , isoscalar scalar σ meson, isoscalar vector ω meson, isovector vector ρ meson, isovector pseudoscalar π meson, and the photon (A) fields [24,30]. Following the standard variational procedure, one can get the equations of motion for nucleons, mesons, and photons, namely the Dirac, Klein-Gordon, and Proca equations, as well as the continuity equation for energy-momentum tensor, from which is derived the system Hamiltonian. In the terms of the creation and annihilation operators ($c_\alpha^\dagger, c_\alpha$) defined by the stationary solutions of the Dirac equation, the Hamiltonian operator can be expressed as

$$H = \sum_{\alpha\beta} c_\alpha^\dagger c_\beta T_{\alpha\beta} + \frac{1}{2} \sum_{\alpha\alpha'\beta\beta'} c_\alpha^\dagger c_\beta^\dagger c_{\beta'} c_{\alpha'} \sum_{\phi} V_{\alpha\beta\alpha'\beta'}^\phi, \quad (1)$$

*longwh@lzu.edu.cn

where $T_{\alpha\beta}$ is the kinetic energy and the two-body terms $V_{\alpha\beta\alpha'\beta'}^\phi$ correspond with the meson- (or photon-) nucleon couplings denoted by ϕ ,

$$T_{\alpha\beta} = \int d\mathbf{r} \bar{\psi}_\alpha(\mathbf{r})(-i\boldsymbol{\gamma} \cdot \nabla + M)\psi_\beta(\mathbf{r}), \quad (2)$$

$$V_{\alpha\beta\alpha'\beta'}^\phi = \int d\mathbf{r} d\mathbf{r}' \bar{\psi}_\alpha(\mathbf{r})\bar{\psi}_{\beta'}(\mathbf{r}')\Gamma_\phi(\mathbf{r}, \mathbf{r}') \\ \times D_\phi(\mathbf{r}, \mathbf{r}')\psi_{\beta'}(\mathbf{r}')\psi_{\alpha'}(\mathbf{r}). \quad (3)$$

In the above equations, $\Gamma_\phi(x, x')$ represent the interaction matrices associated with the σ -scalar, ω -vector, ρ -vector, ρ -tensor, ρ -vector-tensor, π -pseudovector, and photon-vector couplings, $D_\phi(\mathbf{r}, \mathbf{r}')$ denotes the relevant meson (photon) propagator, and M is the nucleon mass (for details, see Refs. [23,24,30]).

Standing on the level of relativistic Hartree-Fock (RHF) approach, the contributions from the negative energy states in the Hamiltonian (1) are neglected as usual, i.e., the so-called no-sea approximation [30]. The Hartree-Fock ground state $|\Phi_0\rangle$ is then determined and consequently the energy functional E is derived, i.e., the expectation of Hamiltonian with respect to $|\Phi_0\rangle$:

$$|\Phi_0\rangle = \prod_{i=1}^A c_i^\dagger |0\rangle, \quad E = \langle \Phi_0 | H | \Phi_0 \rangle, \quad (4)$$

where the index i denotes the positive energy states and $|0\rangle$ is the vacuum state. In the energy functional E , the two-body interactions V^ϕ lead to two types of contributions, i.e., the direct (Hartree) and exchange (Fock) terms. Within RHF [23], the mean field part contains both types of the contributions, i.e., the RHF approach [31], whereas within RHB the Fock terms are neglected just for simplicity.

For the open-shell nuclei, the pairing correlations, which lead to valence particles spreading over the orbits around the Fermi level, have to be taken into account. Unlike the simple BCS method [32], the Bogoliubov theory can unify the descriptions of mean field and pairing correlations in terms of Bogoliubov quasiparticles. It is of special significance in exploring the nuclei far from the β -stability line where the continuum effects become essential and the simple BCS method may break down. In prior studies with both RHB and RHF theories, it has been demonstrated that the scattering of the Cooper pairs into the continuum plays an essential role in the formation of the halo structures [13,14,19].

Following the standard procedure of the Bogoliubov transformation [33,34], the RHF equation can be derived as

$$\int d\mathbf{r}' \begin{pmatrix} h(\mathbf{r}, \mathbf{r}') & \Delta(\mathbf{r}, \mathbf{r}') \\ -\Delta(\mathbf{r}, \mathbf{r}') & h(\mathbf{r}, \mathbf{r}') \end{pmatrix} \begin{pmatrix} \psi_U(\mathbf{r}') \\ \psi_V(\mathbf{r}') \end{pmatrix} \\ = \begin{pmatrix} \lambda + E_q & 0 \\ 0 & \lambda - E_q \end{pmatrix} \begin{pmatrix} \psi_U(\mathbf{r}) \\ \psi_V(\mathbf{r}) \end{pmatrix}, \quad (5)$$

where ψ_U and ψ_V are the quasiparticle spinors, E_q denotes the single quasiparticle energy, and the chemical potential λ is introduced to keep the particle number on the average. For the single-particle Hamiltonian $h(\mathbf{r}, \mathbf{r}')$, it consists of three parts: the kinetic energy h^{kin} , local potential h^D , and nonlocal

TABLE I. Details for the effective interactions PKA1, PKO2, PKO3, PKDD, DDME2, PK1, and NL2. The abbreviations DD and NL denote the density-dependent meson-nucleon couplings and the nonlinear self-couplings, respectively.

	DD	NL	Fock term	π	ρ tensor
PKA1	Yes	No	Yes	Yes	Yes
PKO2	Yes	No	Yes	No	No
PKO3	Yes	No	Yes	Yes	No
PKDD	Yes	No	No	No	No
DD-ME2	Yes	No	No	No	No
PK1	No	Yes	No	No	No
NL2	No	Yes	No	No	No

potential h^E ,

$$h^{\text{kin}}(\mathbf{r}, \mathbf{r}') = \gamma^0 (\boldsymbol{\gamma} \cdot \mathbf{p} + M) \delta(\mathbf{r} - \mathbf{r}'), \quad (6a)$$

$$h^D(\mathbf{r}, \mathbf{r}') = [\Sigma_T(\mathbf{r})\gamma_5 + \Sigma_0(\mathbf{r}) + \gamma^0 \Sigma_S(\mathbf{r})] \delta(\mathbf{r} - \mathbf{r}'), \quad (6b)$$

$$h^E(\mathbf{r}, \mathbf{r}') = \begin{pmatrix} Y_G(\mathbf{r}, \mathbf{r}') & Y_F(\mathbf{r}, \mathbf{r}') \\ X_G(\mathbf{r}, \mathbf{r}') & X_F(\mathbf{r}, \mathbf{r}') \end{pmatrix}. \quad (6c)$$

Details are given in Refs. [23,30]. The pairing potential in the RHF equation (5) reads as

$$\Delta_\alpha(\mathbf{r}, \mathbf{r}') = -\frac{1}{2} \sum_\beta V_{\alpha\beta}^{pp}(\mathbf{r}, \mathbf{r}') \kappa_\beta(\mathbf{r}, \mathbf{r}'), \quad (7)$$

with the pairing tensor κ

$$\kappa_\alpha(\mathbf{r}, \mathbf{r}') = \psi_{V_\alpha}(\mathbf{r})^* \psi_{U_\alpha}(\mathbf{r}'). \quad (8)$$

For the pairing interaction V^{pp} , it is generally taken as a phenomenological form with great success in RHB theory [16,35] and conventional HFB theory [36,37]. In this work, we utilize the finite-range Gogny force D1S [38] with additional strength factor f as the effective pairing interaction,

$$V(\mathbf{r}, \mathbf{r}') = f \sum_{i=1,2} e^{[(r-r')/\mu_i]^2} (W_i + B_i P^\sigma - H_i P^\tau \\ - M_i P \sigma P^\tau), \quad (9)$$

where μ_i , W_i , B_i , H_i , M_i ($i = 1, 2$) are the Gogny parameters and the factor f is adjusted to provide better overall description for the selected carbon isotopes.

Due to the numerical difficulties originating from both RHF mean field and finite-range pairing interactions, the integrodifferential RHF equation (5) is solved by expanding the quasiparticle spinors on the Dirac-Woods-Saxon (DWS)

TABLE II. Blocked quasineutron (ν) orbits of the ground states of the odd carbon isotopes $^{15,17,19,21}\text{C}$ determined by the calculations of PKA1, PKO2, PKO3, PKDD, DD-ME2, PK1, and NL2.

	PKA1	PKO2	PKO3	PKDD	DD-ME2	PK1	NL2
^{15}C	$\nu s_{1/2}$	$\nu d_{5/2}$	$\nu d_{5/2}$	$\nu s_{1/2}$	$\nu s_{1/2}$	$\nu s_{1/2}$	$\nu s_{1/2}$
^{17}C	$\nu s_{1/2}$						
^{19}C	$\nu d_{5/2}$	$\nu s_{1/2}$					
^{21}C	$\nu s_{1/2}$						

TABLE III. The root mean square deviations (MeV) from the data [44] for the binding energies E_b and single- (S_n) and two-neutron (S_{2n}) separation energies of the carbon isotopes. The results are extracted from the calculations by PKA1, PKO2, PKO3, PKDD, DD-ME2, PK1, and NL2 with different pairing strength factor f . See the text for details.

f	PKA1			PKO2			PKO3			PKDD			DD-ME2			PK1			NL2		
	E_b	S_n	S_{2n}	E_b	S_n	S_{2n}	E_b	S_n	S_{2n}	E_b	S_n	S_{2n}									
1.00	1.34	0.88	0.81	2.14	0.43	1.02	2.10	0.65	1.66	2.83	0.78	1.72	3.00	0.97	1.92	1.38	0.71	1.42	12.29	1.77	3.87
1.10	1.58	0.78	0.75	1.78	0.41	0.84	1.35	0.59	1.72	2.46	0.65	1.59	2.49	0.78	1.71	0.90	0.66	1.28	11.18	1.64	3.59
1.15	1.71	0.95	1.10	1.43	0.46	0.80	0.90	0.62	1.79	2.17	0.63	1.52	2.29	0.63	1.68	0.60	0.78	1.27	10.54	1.57	3.43
1.20	2.08	1.03	1.22	1.02	0.55	0.81	0.51	0.69	1.80	1.81	0.66	1.48	1.90	0.64	1.73	0.46	0.80	1.27	9.83	1.51	3.25
1.25	2.60	1.14	1.34	0.65	0.67	0.99	0.67	0.79	1.79	1.38	0.72	1.57	1.45	0.68	1.80	0.81	0.92	1.44	9.05	1.46	3.05

basis [39], which can provide appropriate asymptotic behaviors for the continuum states in the weakly bound nuclei. For the calculations of carbon isotopes, the DWS basis parameters are taken as follows: the spherical box size is fixed to 30 fm and consistently the numbers of basis states with positive and negative energies are chosen as 48 and 12, respectively.

In this work, we performed systematic calculations for the carbon isotopes from ^{10}C to ^{22}C with the RHFB and RHB theories, utilizing the effective interactions with density-dependent meson couplings, namely PKA1 [24], PKO2 [25] and PKO3 [25], PKDD [40] and DD-ME2 [41], and the ones with nonlinear self-couplings, PK1 [40] and NL2 [42]. The details of the selected effective Lagrangians are shown in Table I. For the odd carbon isotopes, the blocking effects are taken into account. In general, e.g., under the BCS scheme, several orbits around the Fermi surface are blocked separately and the blocking with the strongest binding corresponds to the ground state [43]. In present study, the self-consistent calculations are carried out within the Bogoliubov scheme and naturally the blocking effects are considered under the same scheme to keep the consistency of the theory. According to the mapping relation between the HF single-particle and Bogoliubov quasiparticle states (see Fig. 11 in Ref. [17]), the blocked quasiparticle orbit can be determined as the lowest

ones, e.g., the orbits $1s_{1/2}$ or $1d_{5/2}$ for $^{15,17,19,21}\text{C}$. Table II shows the blocking configurations for the ground states of the odd carbon isotopes close to the neutron drip line.

III. RESULTS AND DISCUSSION

To get appropriate pairing effects, first the systematical calculations with different pairing strength factors are performed for the carbon isotopes. Table III shows the root mean square deviations from the data [44] for the binding energies E_b and single- (S_n) and two-neutron (S_{2n}) separation energies extracted from the calculations with the selected effective Lagrangians in Table I. It is found that all the effective interactions present appropriate agreement with the data, except NL2, which fails to provide enough binding for carbon isotopes with about 10% deviations. It can be also seen that the systematics on single- and two-neutron separation energies are improved quantitatively with the modified pairing interactions. Referred to the single-neutron separation energy S_n , the optimized strength factors are determined as $f = 1.1$ for PKA1, PKO2, and PKO3, $f = 1.15$ for PKDD, DD-ME2, and PK1, and $f = 1.25$ for NL2. Among the selected effective Lagrangians, one can find in Table III that PKO2 provides the best agreement with the data on both S_n and S_{2n} , which may imply the most reliable systematics.

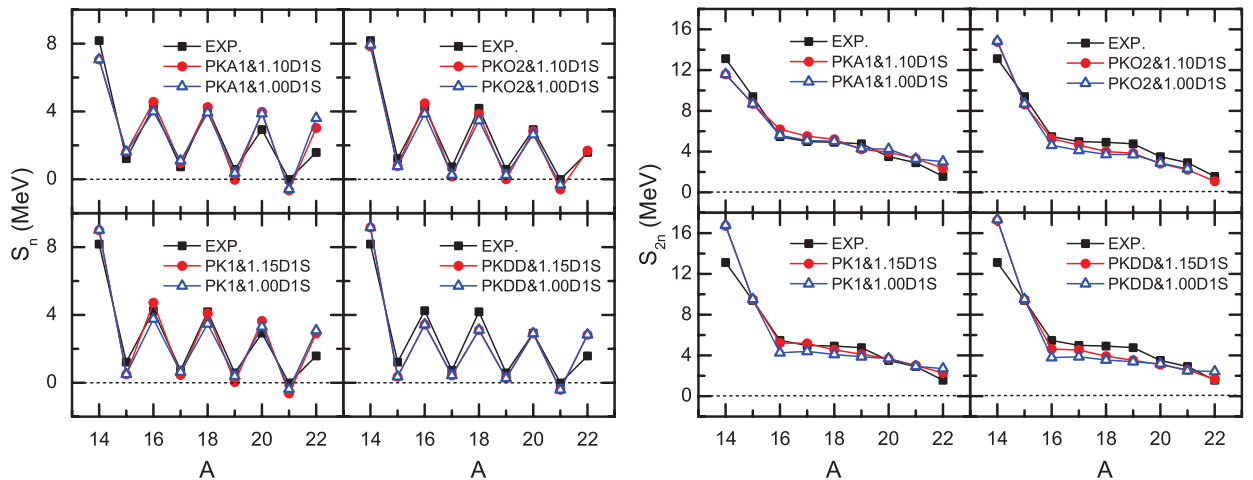


FIG. 1. (Color online) Single-neutron (S_n ; left panels) and two-neutron (S_{2n} ; right panels) separation energies for carbon isotopes from ^{14}C to ^{22}C . The results are calculated by RHFB with PKA1 and PKO2 (upper panels) and by RHB with PK1 and PKDD (lower panels). The filled circles and open upward-pointing triangles denote the results calculated by taking the Gogny force DIS with and without optimized strength factor as the effective pairing interactions, respectively. The data extracted from Ref. [44] are shown in filled squares.

Figure 1 presents the single-neutron separation energies S_n (left panels) and two-neutron ones S_{2n} (right panels) of carbon isotopes calculated with PKA1, PKO2, PK1, and PKDD as compared to the data (filled squares) [44]. The comparison is performed between the calculations with the original effective pairing interaction Gogny-D1S (open upward-pointing triangles) and the ones with the optimized strength factor f (filled circles). From Fig. 1 one can find that the modification on the pairing force brings some systematical improvements on both S_n and S_{2n} , especially for the calculations with PKA1 and PKO2. The results calculated by PKO3 and DD-ME2 are omitted because of the similar systematics with PKO2 and PKDD, respectively. Specifically with the original Gogny-D1S, PKO2 cannot reproduce the drip line ^{22}C , which becomes bound with enhanced pairing force (see Fig. 1). Combined with the results in Table III, we utilize PKO2 with optimized pairing force as the representative to analyze the detailed structure properties of carbon isotopes in the following discussions.

Aiming at the possible halo structure in carbon isotopes, Fig. 2 shows the neutron and proton density distributions provided by PKO2 calculations for even [plot (a)] and odd [plot (b)] carbon isotopes. As shown in Fig. 2(a), it seems that the neutron densities of the even isotopes tend to be more diffuse but not distinct enough to support the occurrence of a halo structure when close to the drip line. From the recent data [44] the two-neutron separation energy of ^{22}C is 1.56 MeV, which implies that the last two valence neutrons are still bound too deeply to spread over a fairly wide range. Hence ^{22}C may not be a good candidate of well-developed two-neutron halo structure. However, in Fig. 2(b) distinct evidence is presented to demonstrate the halo occurrences in ^{17}C and ^{19}C , i.e., more diffused neutron distributions with less neutrons than

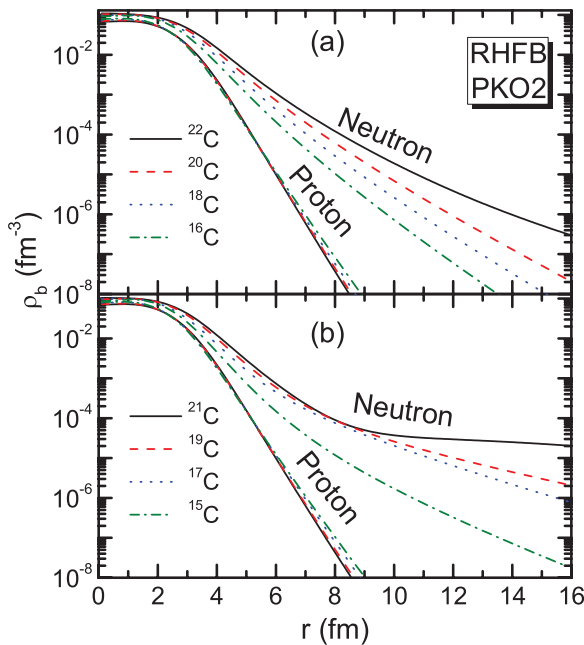


FIG. 2. (Color online) Neutron and proton density distributions for even [plot (a)] and odd [plot (b)] carbon isotopes. The results are calculated by RHFb with PKO2 and the optimized pairing strength factor is adopted as $f = 1.10$. See the text for details.

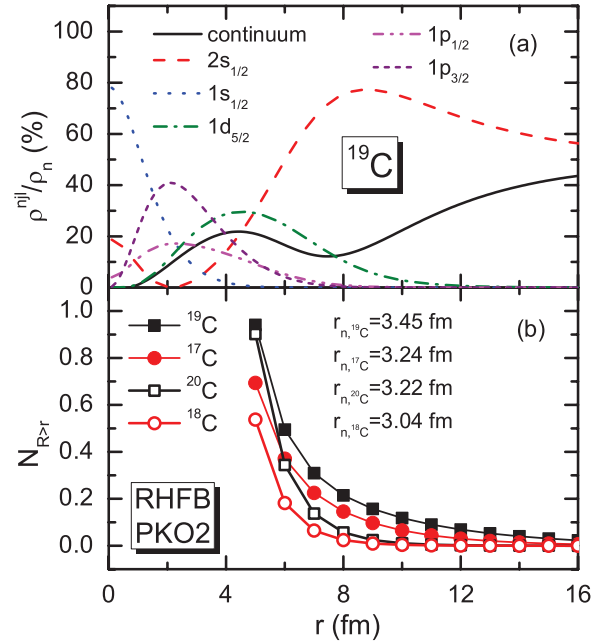


FIG. 3. (Color online) Contributions to neutron density (ρ_n) from (a) canonical neutron orbits (ρ^{nlj}) and the continuum in ^{19}C and (b) neutron numbers ($N_{R>r}$) beyond the sphere with radius r for ^{17}C , ^{18}C , ^{19}C , and ^{20}C . The results are extracted from the calculations of RHFb with PKO2. $r_{n,17\text{C}}$, $r_{n,18\text{C}}$, $r_{n,19\text{C}}$, and $r_{n,20\text{C}}$ denote the root mean square neutron radii of ^{17}C , ^{18}C , ^{19}C , and ^{20}C , respectively.

^{22}C . In fact, strong evidence of the halo occurrence in ^{19}C can be found from the parallel momentum distribution of ^{18}C after the breakup of ^{19}C [6]. As shown in Fig. 1, nearly zero single-neutron separation energies of ^{17}C and ^{19}C can be also treated as more evidence for the existence of a single-neutron halo structure. For ^{21}C the negative value of S_n leads to a diverged matter distribution, which might not be a bound nucleus.

To further illustrate the halo occurrence, Fig. 3(a) presents the contributions to the neutron density from different canonical single-particle orbits. It is clearly shown that the dilute matter distribution at large radial distance is dominated by low- j state $2s_{1/2}$ and the continuum, in accordance with the evidence of halo occurrences in ^{11}Li [13] and Ca isotopes [18]. Consistently Fig. 3(b) presents other direct evidence, i.e., the number of neutrons $N_{R>r}$ located beyond the sphere with radius r . From Fig. 3(b) it can be determined that there exist evident single-neutron halo structures in $^{17,19}\text{C}$ due to fairly large amount of neutrons spreading far beyond the neutron radii r_n . In contrast the values of $N_{R>r}$ in neutron-richer isotopes $^{18,20}\text{C}$ drop sharply with the increase of radius r , consistent with the neutron distributions shown in Fig. 2(a). Combined with the results in Fig. 3(a), one can find that both canonical state $2s_{1/2}$ and the continuum present substantial contributions in the formation of halo, while dominated by the formal one because of its zero centrifugal barrier.

As the complemented demonstration, Figure 4 shows the neutron canonical single-particle energies for the carbon isotopes from ^{15}C to ^{22}C , where the lengths of the ultrathick bar denote the occupation probabilities in half. From Fig. 4

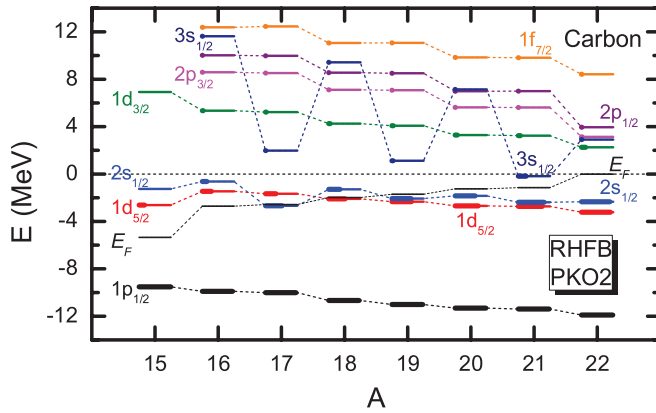


FIG. 4. (Color online) Canonical neutron single-particle energies for carbon isotopes. The results are extracted from the RHF B calculations with PKO2. The lengths of thick bars correspond with the occupation probabilities of neutron orbits in half and E_F represent the Fermi levels.

one can find that the valence orbits $2s_{1/2}$ and $1d_{5/2}$ are close to each other and such high level density in general leads to strong pairing effects. Although both valence orbits are fairly close to the continuum limit, the self-consistent RHF B and RHB calculations only support $^{17,19}\text{C}$ as the candidates of halo nuclei instead of even drip-line isotope ^{22}C , which can be well understood from the blocking effects discussed later.

It should be mentioned that the canonical single-particle states in Fig. 4 are determined from the diagonalization of the density matrix constructed in the Bogoliubov quasiparticle space. In the calculations of $^{17,19}\text{C}$ with PKO2, the neutron quasiparticle states near the Fermi surface are blocked, namely the lowest one, $1s_{1/2}$. According to the mapping relation between the Bogoliubov quasiparticle and canonical single-particle states [15,17], the corresponding contributions of the blocked quasineutron orbits will be mainly mapped into the canonical ones near the Fermi surface, i.e., the canonical $2s_{1/2}$ and $3s_{1/2}$ states, as shown in Fig. 4. Compared to the even isotopes, the neutron staying on the canonical orbit $2s_{1/2}$ then becomes much less bound in the odd carbons due to lack of the extra binding from pairing correlations, which is also illustrated by nearly zero values of S_n in Fig. 1. As a result, the probability density of the valence state $2s_{1/2}$ tends to be much more diffuse than those in even isotopes

to develop the halo structure in $^{17,19}\text{C}$. Due to the blocking of s orbit, the continuum effects are also enhanced relatively in the odd isotopes because the neutron Cooper pairs in $d_{5/2}$ orbit can be only scattered into the continuum by pairing correlations. In addition, the odd-even staggering on the position of the canonical state $3s_{1/2}$ (see Fig. 4) can be also interpreted as blocking effects. In the odd carbon isotopes, the odd quasineutron can be mapped partially into the canonical $3s_{1/2}$ orbits while still visible, e.g., $v^2 = 0.034$ for ^{19}C . As a result, relatively enhanced couplings with the core will remarkably lower the $3s_{1/2}$ orbit. In even isotopes, the pairing correlations constrain the valence neutrons, spreading mostly over the valence orbits $2s_{1/2}$ and $1d_{5/2}$, and fewer neutrons can be scattered into the $3s_{1/2}$ states in the continuum, e.g., $v^2 = 0.004$ for ^{20}C , which therefore become high-lying ones.

As we know, the pairing correlations play significant roles in the halo occurrences for the even nuclear systems, not only in stabilizing the nucleus itself but also in developing the halos by scattering the Cooper pairs into the low-lying s or p orbits. The typical examples are ^{11}Li , the drip-line isotopes of Ca, Zr, and Ce. For the even carbons, particularly ^{22}C , it seems that the extra binding from the pairing correlations makes the s orbit too bound to get dilute matter distribution, which also leads to a fairly large two-neutron separation energy S_{2n} (see Fig. 1). In contrast, for $^{17,19}\text{C}$, due to the absence of extra pairing binding, the odd neutron in the s orbit presents a substantial contribution in the formation of halo structure, which also results in the OES on the neutron radii of carbon isotopes.

Before discussing the OES of neutron radii, it is worthwhile to check the quantitative precision for the theoretical description of the radius. Table IV shows the matter radii of neutron-rich carbon isotopes obtained from the calculations of PKA1, PKO2, PKO3, PKDD, DD-ME2, and PK1, as compared to the experimental data [45,46]. It is found that both RHF B and RHB calculations with the selected effective Lagrangians provide appropriate agreement with the data, which to some extent demonstrates the theoretical reliability.

In fact not only for the total ones, the selected effective Lagrangians with optimized pairing forces also present proper quantitative descriptions for the neutron radii. As shown in Fig. 5(a) and referred to the data [46], the neutron root mean square radii from ^{14}C to ^{22}C are well reproduced by both RHF B and RHB calculations to certain quantitative

TABLE IV. Matter radii (fm) for carbon isotopes extracted from the calculations of PKA1, PKO2, PKO3, PKDD, DD-ME2, and PK1, as compared to the experimental data [45,46].

	^{14}C	^{15}C	^{16}C	^{17}C	^{18}C	^{19}C	^{20}C
PKA1	2.53	2.74	2.73	2.89	2.91	3.02	3.08
PKO2	2.43	2.55	2.63	2.92	2.81	3.11	2.97
PKO3	2.47	2.59	2.68	2.91	2.86	3.21	3.02
PKDD	2.43	2.75	2.66	2.91	2.86	3.26	3.03
DD-ME2	2.55	2.68	2.76	2.93	2.94	3.24	3.10
PK1	2.42	2.72	2.65	2.86	2.84	3.06	3.01
Ref. [45]	2.62(6)	2.78(9)	2.76(6)	3.04(11)	2.90(19)	2.74(96)	
Ref. [46]	2.30(7)	2.48(3)	2.70(3)	2.72(3)	2.82(4)	3.13(7)	2.98(5)
		2.50(8)		2.73(4)		3.23(8)	

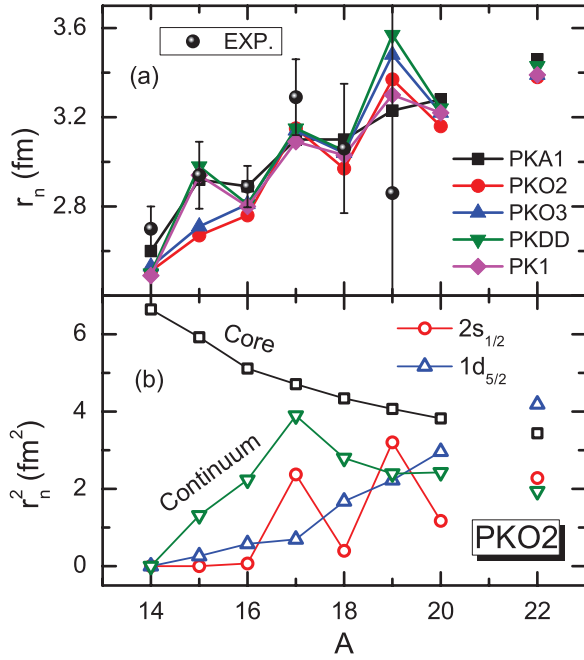


FIG. 5. (Color online) (a) Neutron root mean square radii calculated by RHFB with PKA1, PKO2, and PKO3 and by RHB with PKDD and PK1, as compared with the data [for ^{19}C it reads as 2.86(1.4) fm] [45], and (b) corresponding contributions from the neutron core orbits ($1s_{1/2}$, $1p_{3/2}$, and $1p_{1/2}$), valence orbits ($2s_{1/2}$ and $1d_{5/2}$), and the continuum. The results are provided by the calculations of RHFB with PKO2. See the text for details.

precision. Evidently as shown in Fig. 5(a) all the theoretical calculations present distinct OES on the neutron radii, in accordance with the experimental systematics. Specifically, as seen from Fig. 5(b), such OES is determined by the valence neutrons lying in the canonical orbit $2s_{1/2}$ and also depends on whether the corresponding Bogoliubov quasiparticle s orbit is

blocked. Referring to Table II, one can find that the blocking configurations are consistent with the OES in Fig. 5(a). In ^{15}C , which has larger neutron radius than ^{16}C in the calculations with PKA1, PKDD, and PK1, the quasiparticle s orbit is blocked. Due to a similar reason, and consistent with the halo occurrence, the neutron radii of halo nuclei $^{17,19}\text{C}$ are distinctly larger than those of the even neighbors. The exceptions are the calculations with PKO2 and PKO3 at ^{15}C and the one with PKA1 at ^{19}C , where the neutron radii change smoothly. As seen from Table II such exceptional cases correspond with the blocking of $d_{5/2}$ orbit, in which the odd neutron is localized mostly inside the nucleus by the centrifugal barrier. As a result, the ground state of ^{19}C determined by PKA1 does not correspond with a halo structure since the odd neutron blocks the $d_{5/2}$ orbit, and due to the pairing effects the paired neutrons in the low- j s state are bound too strongly to distribute extensively.

As further illustration of the consistent relation between the OES and blocking configurations, Table V shows the binding energies and neutron radii of $^{15,17,19}\text{C}$ extracted from the self-consistent calculations with the blockings of $s_{1/2}$ and $d_{5/2}$ orbits, respectively. As shown in the lower panel, the blockings of the low- j s orbit in general lead to more extensive neutron distributions, from which are also well demonstrated by the blocking effects in the formation of single-neutron halo structure of $^{17,19}\text{C}$. Specifically for the calculations of ^{19}C with different blocking, the binding energies determined by PKA1 are close to each another and in fact when s orbit is blocked PKA1 also supports the halo occurrence in ^{19}C . In contrast the others present distinct differences in the binding energies, especially for PKO2, which confirms the halo emergence in ground state.

It is well known that pairing correlation plays an important role in stabilizing the finite nuclei, especially the exotic ones. For ^{11}Li , the neutron drip-line isotopes of Ca, Zr, and Ce, it is already demonstrated that the pairing correlations show

TABLE V. Binding energies in MeV (upper panel) and neutron radii in fm (lower panel) for $^{15,17,19}\text{C}$ calculated by the effective Lagrangians PKA1, PKO2, PKO3, PKDD, DD-ME2, and PK1 with different blocking configurations. For each odd isotopes, the first and second rows correspond with blocking neutron (ν) orbits $s_{1/2}$ and $d_{5/2}$, respectively. The bold type denotes the ground states.

	PKA1	PKO2	PKO3	PKDD	DD-ME2	PK1
Binding energies (MeV)						
^{15}C	-107.48	-104.98	-105.95	-105.30	-105.79	-105.91
	-106.63	-105.69	-106.11	-105.23	-105.35	-105.79
^{17}C	-112.99	-110.32	-110.81	-109.83	-110.11	-110.76
	-112.44	-110.06	-110.30	-109.30	-109.50	-110.21
^{19}C	-117.03	-114.17	-114.43	-113.35	-113.21	-114.78
	-117.21	-113.13	-113.65	-112.72	-112.71	-114.16
Neutron radii (fm)						
^{15}C	2.92	3.05	2.99	2.98	2.93	2.94
	2.66	2.67	2.71	2.70	2.72	2.88
^{17}C	3.10	3.15	3.14	3.15	3.16	3.09
	3.04	2.91	2.98	2.99	3.04	2.97
^{19}C	3.42	3.37	3.48	3.57	4.20	3.31
	3.23	4.85	3.43	3.31	3.60	3.19

positive effects in both stabilizing and developing the halo structures. In the RHF and RHB calculations of $^{17,19}\text{C}$, the quasiparticle s orbit is blocked and the corresponding contributions are mainly mapped to the canonical orbit $2s_{1/2}$, which plays the dominate role in the single-neutron halo formation of $^{17,19}\text{C}$. This implies that the unpaired odd neutron in low- j orbit may also contribute to develop a halo structure when it is not so deeply bound. From previous analysis it is just due to the lack of extra binding from the pairing correlations that the odd neutron in s orbit can spread far beyond the center of nucleus.

IV. SUMMARY AND PERSPECTIVES

In this work we have systematically calculated the carbon isotopes using the relativistic Hartree-Fock-Bogoliubov theory with PKA1, PKO2, and PKO3 as well as the relativistic Hartree-Bogoliubov theory with PKDD, DD-ME2, PK1, and NL2. It is found that with the optimized pairing force the selected effective Lagrangians except NL2 can properly describe the structural properties of the carbon isotopes, e.g., reproducing the binding energies and matter radii by certain quantitative precision. Specifically, distinct evidence has demonstrated the single-neutron halo occurrences in $^{17,19}\text{C}$, as well as the odd-even staggering (OES) of neutron radii in the vicinity of the neutron drip line. The self-consistent RHF and RHB calculations do not support the emergence of two-neutron halo structure in ^{22}C as indicated by the experimental reaction cross-sectional measurement [9]. Further detailed analysis shows that the halo emergences in $^{17,19}\text{C}$, as well as the OES of neutron radii, are essentially concerned with the blocking effects in the odd carbon isotopes. Unlike the even nuclear

systems, in which the pairing correlations play significant roles in both developing and stabilizing the halo structures, the unpaired odd neutron in a weakly bound low- j s orbit dominates the halo formation in $^{17,19}\text{C}$ as well as reproduces the OES of neutron radii for the drip-line carbon isotopes.

It should be noticed that for the odd carbons the blocking treatment in this work is just the first-order evaluation of the blocking effects, and the current effects induced by the odd neutron are neglected as well. In addition, due to the limit of the present theoretical platform, we only performed the spherical calculations for the carbon isotopes within the relativistic Hartree and Hartree-Fock theories, while some carbon isotopes are potentially deformed. After considering the shape fluctuations in both β and γ deformations, the average neutron quadrupole deformations ($\langle\beta\rangle_n, \langle\gamma\rangle_n$) of $^{16,18,20}\text{C}$ are $(0.50, 21^\circ)$, $(0.49, 29^\circ)$, and $(0.50, 21^\circ)$, respectively [47]. It is then expected that the shape fluctuations will bring some influence on the structure properties of the carbon isotopes, especially in the vicinity of the drip line. Therefore, the self-consistent treatment of the deformation as well as the odd-particle effects is expected to be considered carefully for more reliable description of carbon isotopes.

ACKNOWLEDGMENTS

This work is partly supported by the National Science Foundation of China under Grants No. 11075066 and No. 11205075, the Fundamental Research Funds for the Central Universities under Contracts No. lzujbky-2012-k07 and No. lzujbky-2012-7, and the Program for New Century Excellent Talents in University.

-
- [1] L. Chulkov, G. Kraus, O. Bochkarev *et al.*, *Nucl. Phys. A* **603**, 219 (1996).
- [2] A. C. Mueller, *Prog. Part. Nucl. Phys.* **46**, 359 (2001).
- [3] I. Tanihata, T. Kobayashi, O. Yamakawa *et al.*, *Prog. Part. Nucl. Phys.* **35**, 505 (1995).
- [4] J. P. Schiffer, S. M. Austin, P. Schuck *et al.*, *Nuclear Physics: The Core of Matter, the Fuel of Stars* (National Academies Press, Washington, DC, 1999).
- [5] I. Tanihata, H. Hamagaki, O. Hashimoto, Y. Shida *et al.*, *Phys. Rev. Lett.* **55**, 2676 (1985).
- [6] D. Bazin, W. Benenson, B. A. Brown *et al.*, *Phys. Rev. C* **57**, 2156 (1998).
- [7] D. Q. Fang, T. Yamaguchi, T. Zheng *et al.*, *Phys. Rev. C* **69**, 034613 (2004).
- [8] W. Horiuchi and Y. Suzuki, *Phys. Rev. C* **74**, 034311 (2006).
- [9] K. Tanaka, T. Yamaguchi, T. Suzuki *et al.*, *Phys. Rev. Lett.* **104**, 062701 (2010).
- [10] M. Sharma, A. Bhagwat, Z. A. Khan, W. Haider and Y. K. Gambhir, *Phys. Rev. C* **83**, 031601 (2011).
- [11] L. Lu-Lu, J. Meng, P. Ring, Z. En-Guang, and S.-G. Zhou, *Chin. Phys. Lett.* **29**, 042101 (2012).
- [12] H. T. Fortune and R. Sherr, *Phys. Rev. C* **85**, 027303 (2012).
- [13] J. Meng and P. Ring, *Phys. Rev. Lett.* **77**, 3963 (1996).
- [14] J. Meng and P. Ring, *Phys. Rev. Lett.* **80**, 460 (1998).
- [15] J. Meng, *Nucl. Phys. A* **635**, 3 (1998).
- [16] D. Vretenar, A. V. Afanasjev, G. A. Lalazissis, and P. Ring, *Phys. Rep.* **409**, 101 (2005).
- [17] J. Meng, H. Toki, S.-G. Zhou *et al.*, *Prog. Part. Nucl. Phys.* **57**, 470 (2006).
- [18] J. Meng, H. Toki, J. Y. Zeng, S. Q. Zhang, and S. G. Zhou, *Phys. Rev. C* **65**, 041302 (2002).
- [19] W. H. Long, P. Ring, J. Meng, N. Van Giai, and C. A. Bertulani, *Phys. Rev. C* **81**, 031302 (2010).
- [20] M. Grasso, S. Yoshida, N. Sandulescu, and N. Van Giai, *Phys. Rev. C* **74**, 064317 (2006).
- [21] J. Meng, K. Sugawara-Tanabe, S. Yamaji, and A. Arima, *Phys. Rev. C* **59**, 154 (1999).
- [22] W. Zhang, J. Meng, S. Zhang *et al.*, *Nucl. Phys. A* **753**, 106 (2005).
- [23] W. H. Long, P. Ring, N. Van Giai, and J. Meng, *Phys. Rev. C* **81**, 024308 (2010).
- [24] W. H. Long, H. Sagawa, N. V. Giai, and J. Meng, *Phys. Rev. C* **76**, 034314 (2007).
- [25] W. H. Long, H. Sagawa, J. Meng, and N. V. Giai, *Europhys. Lett.* **82**, 12001 (2008).
- [26] W. H. Long, T. Nakatsukasa, H. Sagawa *et al.*, *Phys. Lett. B* **680**, 428 (2009).

- [27] W. H. Long, H. Sagawa, J. Meng, and N. V. Giai, *Phys. Lett. B* **639**, 242 (2006).
- [28] H. Liang, W. H. Long, J. Meng, and N. V. Giai, *Eur. Phys. J. A* **44**, 119 (2010).
- [29] H. Liang, N. Van Giai, and J. Meng, *Phys. Rev. Lett.* **101**, 122502 (2008).
- [30] A. Bouyssy, J.-F. Mathiot, N. Van Giai, and S. Marcos, *Phys. Rev. C* **36**, 380 (1987).
- [31] W. H. Long, N. V. Giai, and J. Meng, *Phys. Lett. B* **640**, 150 (2006).
- [32] J. Bardeen, L. N. Cooper, and J. R. Schrieffer, *Phys. Rev. C* **106**, 162 (1957).
- [33] L. Gor'kov, *Sov. Phys. JETP* **7**, 505 (1958).
- [34] H. Kucharek and P. Ring, *Z. Phys. A* **339**, 23 (1991).
- [35] T. Gonzalez-Llarena, J. L. Egidio, G. A. Lalazissis, and P. Ring, *Phys. Lett. B* **379**, 13 (1996).
- [36] J. Dechargé and D. Gogny, *Phys. Rev. C* **21**, 1568 (1980).
- [37] J. Dobaczewski, H. Flocard, and J. Treiner, *Nucl. Phys. A* **422**, 103 (1984).
- [38] J. F. Berger, M. Girod, and D. Gogny, *Nucl. Phys. A* **428**, 23 (1984).
- [39] S.-G. Zhou, J. Meng, and P. Ring, *Phys. Rev. C* **68**, 034323 (2003).
- [40] W. H. Long, J. Meng, N. Van Giai, and S.-G. Zhou, *Phys. Rev. C* **69**, 034319 (2004).
- [41] G. A. Lalazissis, T. Niksic, D. Vretenar, and P. Ring, *Phys. Rev. C* **71**, 024312 (2005).
- [42] S.-J. Lee, J. Fink, A. B. Balantekin *et al.*, *Phys. Rev. Lett.* **57**, 2916 (1986).
- [43] J. Li, Z. Ma, B. Chen, and Y. Zhou, *Phys. Rev. C* **65**, 064305 (2002).
- [44] G. Audi and W. Meng (private communication).
- [45] E. Liatard, J. Bruandet, F. Glasser *et al.*, *Europhys. Lett.* **13**, 401 (1990).
- [46] A. Ozawa, O. Bochkarev, L. Chulkov *et al.*, *Nucl. Phys. A* **691**, 599 (2001).
- [47] J. Yao, J. Meng, P. Ring, Z. X. Li, Z. P. Li, and K. Hagino, *Phys. Rev. C* **84**, 024306 (2011).